NASA TECHNICAL TRANSLATION NASA TT - 20310

CALCULATION OF NON-STATIONARY AERODYNAMIC FORCES IN THE NEAR SONIC RANGE

I. Teipel

Translation of "Die Berechnung Instationaerer Luftkraefte im Schallnahen Bereich", Journal de Mecanique, vol. 4, no. 3, Sept. 1965, pp 335-360

(NASA-TT-20310) CALCULATION OF NON-STATIONARY AERODYNAMIC FORCES IN THE NEAR SONIC RANGE (NASA) 25 p CSCL 01A

N88-29782

Unclas
G5/02 0161730

NATIONAL AERONAUTICS AND SPACE ADMINISTRATION
WASHINGTON, D. C. 20546 AUGUST 1988

NASA National Aeronautics and Space Administration

Report Documentation Page

1. Report No.	2. Government Accession No.	3. Recipient's Catalog No.
TT-20310		

4. Title and Subtitle	5. Report Date
CALCULATION OF NON-STATIONARY AERODYNAMIC FORCES IN THE NEAR SONIC RANGE	AUGUST 1988
	6. Performing Organization Code

7. Author(s)	8. Performing Organization Report No.
I. Teipel	10. Work Unit No.

9. Performing Organization Name and Address	11. Contract or Grant No.
National Aeronautics and Space Administration Washington, DC 20546	NASW-4307
	13. Type of Report and Period Covered
12. Sponsoring Agency Name and Address	translation
NASA - LEWIS RESEARCH CENTER	14. Sponsoring Agency Code

15. Supplementary Notes

Transl. from GERMAN to ENGLISH of "Die Berechnung Instationaerer Luftkraefte im Schallnahen Bereich", Journal de Mecanique, Vol. 4, No. 3, Sept. 1965, pp 335-360

Transl. by SCITRAN, Santa Barbara, CA 93150.

16. Abstract

Development of a mathematical method for calculating nonstationary supersonic flow in the near sonic range. A perturbation formula is derived based on the exact stationary values; it is applicable to the equation for potential. The problem can thus be divided into stationary and nonstationary fields. The pressure distribution in an oscillating profile is determined, based on hyperbolic differential equations. It is shown that there are important corallaries concerning the application of linear theory. With suitable extrapolations, linear theory can be used up to about Mach 0.8. Linear theory is not applicable, however, when determining the moment coefficients; for this case, a special technique is described.

17. Key Words (Suggested by Author(s))	18. Distribution Statement
	unclassified-unlimited

19. Security Classif. (of this report)	20. Security Classif. (of this page)	21. No. of pages	22. Price
unclassified	unclassified	29	

NASA FORM 1626 OCT 86

Calculation of Non-stationary Aerodynamic Forces in the Near-Sonic Range

by I. Teipel

Institute für Theoretische Gasdynamik der Deutschen Versuchsanstalt für Luft und Raumfahrt, Aachen, West Germany.

1. Introduction

The assumptions under which the equations for non-stationary flow can be linearized about a slender, oscillating profile were derived in [1]. The result was that the theory of small perturbations leads to linear differential equations, except in the transsonic and hypersonic regimes. Indeed, for sufficiently high reduced frequencies it is possible even in the near-sonic regime to make calculations using a linearized theory. For vanishing reduced frequencies, however, the near-sonic, stationary, nonlinear differential equations must be taken as the limiting case.

When the Mach number is very large, that is in the hypersonic region, a strong compression shock is joined to a sharp profile. At this point the pressure perturbations are no longer small. Even entropy changes in the entire zone behind the shock wave must be considered under certain circumstances, according to the degree of curvature of the shock front. A very good approximation theory, the so-called "Kolben Theory", exists for this nonlinear case. Hayes [2] has shown that the flow around a wing at high Mach numbers can be considered to be one-dimensional, even when entropy changes occur in the region behind the shock. Lighthill [3] formulated this result for the oscillating profile, and with it was able to point out a good and quite simple relationship between pressure and speed.

In the second nonlinear regime, no such well-developed method has become known /336
to date. G. Coupry and G. Piazolli [4] have tried to solve this problem using additional

* Numbers in margin indicate foreign pagination

assumptions. A non-stationary component was superimposed on the stationary flow, which was considered as given. The pressure distribution at the profile in the stationary flow was set constant. If a compression shock appears at the bodies – this condition has been dealt with in [4] – then the shock front divides the current surface into two regions, in each of which the stationary part of the pressure is different, though at all times remaining constant. Despite this daring hypothesis, the results agree surprisingly well with experimental measurements. The acceleration potential was introduced in a work by Eckhaus [5] for the solution to this problem. The departure point was similarly a perturbation theory of the non-stationary potential relative to the stationary values. Still further mathematical simplifications are made in order to obtain results. Recently, a work [6] has been published in which the method of local linearization was carried over to non-stationary processes. Similar ideas are mentioned in [7].

A method of characteristics for this near-sonic regime will now be developed. Naturally, the area of applicability is restricted, since this relies on hyperbolic differential equations. But this simply means that in the entire region under consideration the Mach number must exceed one. Exactly as in [4] and [5], non-stationary effects should be superimposed to first order on the values for the stationary flow. In the subsequent examples, parabolic profiles will be investigated, for which the compression shock occurs at the peak.

For encouragement in this work, as well as for worthwhile discussions, I would especially like to thank Prof. Dr. K. Oswatitsch.

2. Fundamental Equations of the Near-Sonic Current

The derivation of the characteristic equations will start with the potential equations. This is advantageous because two consistency relations are then obtained. Of course, an additional integration is necessary. If one proceeds from the three basic equations, one will obtain correspondingly three consistency conditions. Since small

perturbations are assumed, the full potential equation can be simplified. One obtains for the near-sonic regime [8]:

$$\left[1 - M_\infty^2 - (\gamma+1)M_\infty^2 \varphi_x\right]\varphi_{xx} + \varphi_{yy} - \frac{1}{c_\infty^2}\varphi_{tt} - 2\frac{M_\infty}{c_\infty}\varphi_{xt} = 0. \tag{1}$$

Here, $\varphi(x,y,t)$ signifies the velocity potential, M_∞ and c_∞ are the Mach number and sound velocity of the incident flow, and $\gamma = \frac{c_p}{c_v}$ is the ratio of specific heats. For the nonlinear term before φ_{xx}, six different forms exist in the literature [9]; here, the expression proposed in [10] has been chosen. /337

The boundary conditions for the first-order theory are the same as in the linear theory. The descending air distribution on the profile axis, here the x-axis, can be fit by:

$$y = 0: \quad \varphi_y = \frac{1}{U_\infty}\frac{\partial h}{\partial t} + \frac{\partial h}{\partial x}, \tag{2}$$

where $h(x,t)$ is here the profile surface and U_∞ the incident flow velocity. A further boundary condition is now furnished by the compression shock that goes out from the tip of the body. The necessary formulas can be taken from [11]. With this, the mathematical formulation of the problem is given.

The procedure for the solution of eq. (1), as already indicated, should be to superimpose to first order a non-stationary part $\tilde{\Phi}(x,y,t)$ of the potential onto a known stationary part $\Phi(x,y)$. A perturbation theory with respect to the stationary values will be developed. The following formulation then results:

$$\varphi(x,y,t) = \Phi(x,y) + \tilde{\Phi}(x,y,t). \tag{3}$$

On substituting into the potential equation (1), one obtains:

$$\left[1 - M_\infty^2 - (\gamma+1)M_\infty^2 \Phi_x\right] \Phi_{xx} + \Phi_{yy}$$
$$+ \left\{ \left[1 - M_\infty^2 - (\gamma+1)M_\infty^2 \Phi_x\right] \bar{\Phi}_{xx} - (\gamma+1)M_\infty^2 \left(\Phi_{xx} + \underline{\bar{\Phi}_{xx}}\right) \bar{\Phi}_x \right.$$
$$\left. + \bar{\Phi}_{yy} - \frac{1}{c_\infty^2} \bar{\Phi}_{tt} - 2\frac{M_\infty}{c_\infty} \bar{\Phi}_{xt} \right\} = 0. \qquad (4)$$

As could be expected, the stationary problem can be split at the two initial terms. Since only terms of first order in the amplitude functions should be considered, the underlined term in the curved bracket of eq. (4) vanishes. The assumption used is that $\bar{\Phi}_{xx}$ must be small relative to Φ_{xx}. This is implied by the above-mentioned assumptions. The time dependence can be expressed by periodic functions, since oscillating, non-stationary motions are to be investigated. One thus obtains the new expression

$$\varphi(x, y, t) = \Phi(x, y) + \psi(x, y) e^{i\omega t}. \qquad (5)$$

It could now happen that, although the Mach number for the stationary flow field is indeed greater than one, the total Mach number including the non-stationary addition /338 is less than one. For this case the theory is not valid. If with very small supersonic Mach numbers the compression shock is also to lie close to the profile peak, then the perturbation of the stationary field must be very small, though still correct relative to that of the non-stationary field so that the assumption expressed at the start remains statisfied. The closer the Mach number of incident flow approaches $M_\infty = 1$, the less the non-stationary influence can be if this theory is to find application. If eq. (5) is now substituted into eq. (4), the two differential equations result:

$$\left[1 - M_\infty^2 - (\gamma+1)M_\infty^2 \Phi_x\right] \Phi_{xx} + \Phi_{yy} = 0; \qquad (6)$$

$$\left[1 - M_\infty^2 - (\gamma+1)M_\infty^2 \Phi_x\right] \phi_{xx} - (\gamma+1)M_\infty^2 \Phi_{xx} \psi_x + \psi_{yy} + \frac{\omega^2}{c_\infty^2} \psi - 2i\frac{\omega}{U_\infty} M_\infty^2 \psi_x = 0. \qquad (7)$$

These relationships serve as starting equations for the theory of characteristics.

For the boundary conditions, analogous expressions can be given. The profile surface $h(x,t)$ can be split up into two parts, one representing the thickness distribution and another giving the motion of the profile:

$$h(x,t) = h_1(x) + h_2(x)e^{i\omega t} \tag{8}$$

With this one finds for the descending air distribution, after some short recomputations:

$$\Phi_y = \frac{dh_1}{dx}; \tag{9}$$

$$\psi_y = \frac{dh_2}{dx} + i\frac{\omega}{U_\infty}h_2. \tag{10}$$

The conditions which hold over the compression shock will written down in the sections where the special steps of the procedure are dealt with.

3. The stationary flow field

In order to be able to carry out the calculation, it is next necessary to know the stationary flow field. The characteristic equations can be derived without difficulty from the relationships given in [12] for axially symmetric supersonic fields. However, the nonlinear term of the potential equation is given there in a different form from that of eq. (1). Thus, the derivation of the consistency relations will be briefly discussed.

If the procedure that is described, e.g., in [13] is applied, the directional conditions are obtained: /339

$$\left(\frac{\partial y}{\partial x}\right)_{\xi,\eta} = \pm\frac{1}{\sqrt{M_\infty^2 - 1 + (\gamma+1)M_\infty^2\Phi_x}}, \tag{11}$$

where ξ=const. stands for the left-hand (upper sign) characteristic and η=const. stands for the right-hand characteristic. The form under the root is exactly that of the nonlinear term in eq. (1). To find the characteristic form of eq. (6) it must be transformed to the new direction. After a longer, simple calculation the consistency

relation is obtained:

$$\pm\sqrt{M_\infty^2 - 1 + (\gamma+1)M_\infty^2\,\Phi_x}\left(\frac{\partial\Phi_x}{\partial x}\right)_{\xi,\eta} + \left(\frac{\partial\Phi_y}{\partial x}\right)_{\xi,\eta} = 0. \tag{12}$$

It is easy to convince oneself that after performing the differentiation, eq. (6) is once again obtained. These two new differential equations are characterized by the fact that sometimes derivatives exist for only one direction. They may be written in still simpler form if the following quantities are introduced:

$$\begin{cases} \lambda = M_\infty^2 - 1 + (\gamma+1)M_\infty^2\,\Phi_x; \\ \mu = \frac{3}{2}(\gamma+1)M_\infty^2\,\Phi_y. \end{cases} \tag{13}$$

With these relationships eqs. (12) read

$$\left(\frac{\partial\lambda^{\frac{3}{2}}}{\partial x}\right)_{\xi,\eta} \mp \left(\frac{\partial\mu}{\partial x}\right)_{\xi,\eta} = 0, \tag{14}$$

whose solution can be given immediately as

$$\lambda^{\frac{3}{2}} \mp \mu = \text{const}. \tag{15}$$

The constant depends on which characteristic is used. With the new variables the boundary condition reads

$$y = 0: \quad \mu = \frac{3}{2}(\gamma+1)M_\infty^2\,\frac{dh_1}{dx}. \tag{16}$$

A further boundary value is attached to the shock front. For the introduction of a potential rotational freedom must be assumed. That means that the shock wave on the profile can only be very weak. The entropy then changes, to lowest order, as the third power of the shock strength. In this approximation the relationship at the shock poles can be replaced with that at the characteristic. Thus, it is not necessary to use the actual shock poles. The inclination of the shock front in the flow plane can be expressed by means of the Mach line inclination in front of and behind the front. /340

THE SPECIAL STEPS.– For the calculation of the characteristic network it can be useful that, as mentioned above, the consistency relations, eq. (15), retain their validity off and over the shock front. With the assumption that only profiles symmetric about the x-axis are considered, the problem can be restricted to the upper half-plane $y \geq 0$. In figure 1 this means that between P_1 and P_3 and P_2 and P_4, respectively, eq. (15) must apply. In addition, the points P_3 and P_4 should lie in front of the bow wave in the undisturbed current. There are right-hand characteristics, and the relations therefore read

$$\begin{cases} \lambda_1^{\frac{2}{2}} - \lambda_3^{\frac{2}{2}} + \mu_1 - \mu_3 = 0; \\ \lambda_2^{\frac{2}{2}} - \lambda_4^{\frac{2}{2}} + \mu_2 - \mu_4 = 0. \end{cases} \tag{17}$$

Further:

$$\begin{cases} \lambda_3 = \lambda_4 = \lambda_\infty = M_\infty^2 - 1; \\ \mu_3 = \mu_4 = \mu_\infty = 0. \end{cases} \tag{18}$$

If these values are substituted in eqs. (17) and the two equations are subtracted, one obtains:

$$\lambda_1^{\frac{2}{2}} - \lambda_2^{\frac{2}{2}} + \mu_1 - \mu_2 = 0. \tag{19}$$

Since P_1 and P_2 are connected through a left-hand characteristic, the following must additionally hold:

$$\lambda_1^{\frac{2}{2}} - \lambda_2^{\frac{2}{2}} - \mu_1 + \mu_2 = 0. \tag{20}$$

From eqs. (19) and (20) it follows immediately that:

$$\lambda_1 = \lambda_2; \qquad \mu_1 = \mu_2. \tag{21}$$

It can be concluded from this that for the left-handed characteristics the state variables are constant. This occurs very frequently with simple problems of single waves.

a. General Step.– **The general step should now be dealt with. This is characterized by the fact that from two known points P_1 and P_2 (fig. 2) a new point P_3 is calculated. From the expression, eq. (21), the values of λ_3 and μ_3 are identical with**

those of λ_2 and μ_2. It remains only to ascertain the corresponding location of the new point. Between P_1 and P_3 and P_2 and P_3, respectively, the Mach lines can be viewed as pieces of straight lines, whose slopes are given by eq. (11):

$$y_3 - y_1 = -\frac{2}{\sqrt{\lambda_1} + \sqrt{\lambda_3}}(x_3 - x_1); \tag{22}$$

$$y_3 - y_2 = \frac{1}{\sqrt{\lambda_3}}(x_3 - x_2). \tag{23}$$

The mean value of $\sqrt{\lambda}$ for to the two points to be connected is used for the slope of the Mach lines. Thus one finds the space coordinates for P_3

$$\begin{cases} x_3 = \frac{\sqrt{\lambda_3}(\sqrt{\lambda_1}+\sqrt{\lambda_3})}{\sqrt{\lambda_1}+3\sqrt{\lambda_3}}\left[y_1 - y_2 + \frac{2x_1}{\sqrt{\lambda_1}+\sqrt{\lambda_3}} + \frac{x_2}{\sqrt{\lambda_3}}\right]; \\ y_3 = \frac{\sqrt{\lambda_3}(\sqrt{\lambda_1}+\sqrt{\lambda_3})}{\sqrt{\lambda_1}+3\sqrt{\lambda_3}}\left[\frac{2(x_1-x_2)}{\sqrt{\lambda_3}(\sqrt{\lambda_1}+\sqrt{\lambda_3})} + \frac{y_1}{\sqrt{\lambda_3}} + \frac{2y_2}{\sqrt{\lambda_1}+\sqrt{\lambda_3}}\right]. \end{cases} \tag{24}$$

b. Edge step.– Now the characteristic ξ=const. is lost. At the edge point P_3 (fig. 3) on the x-axis, the descending air distribution as a function of x is known. The consistancy relation reads

$$\lambda_3^{\frac{1}{2}} - \lambda_\infty^{\frac{1}{2}} + \mu_3 = 0. \tag{25}$$

In place of the point P_2 one can also, as is done here, include the region of the unperturbed current. The resulting boundary condition is /342

$$\mu_3 = \frac{3}{2}(\gamma+1)M_\infty^2\left(\frac{dh_1}{dx}\right)_3. \tag{26}$$

Since the x coordinate of P_3 is not known *a priori*, still another equation is used, the equation of the Mach lines:

$$y_2 = \frac{2}{\sqrt{\lambda_2} + \sqrt{\lambda_3}}(x_3 - x_2). \tag{27}$$

Additionally, it must be taken into consideration that P_3 lies on $y_3 = 0$. The three last equations form a non-linear system of equations, which can only be solved iteratively. This system will be transformed even further for a special case. For this, the profile contour must be given. In view of the foregoing examples the following is chosen:

$$-1 \le x \le 1: \quad h_1 = \tau(1 - x^2). \tag{28}$$

τ denotes the thickness-chord ratio of the profile. On substituting in eq. (26), one obtains:

$$\mu_3 = -3(\gamma + 1)M_\infty^2 \tau x_3. \tag{29}$$

x_3 is connected with λ_3 by eq. (27). It should therefore be eliminated from eq. (29):

$$\mu_3 = -3(\gamma + 1)M_\infty^2 \tau \left(x_2 + \frac{\sqrt{\lambda_2} + \sqrt{\lambda_3}}{2} y_2 \right). \tag{30}$$

When equations (30) are joined with (25) by substituting for μ_3, a cubic equation for $\sqrt{\lambda_3}$ is arrived at after a few short calculations:

$$\left(\sqrt{\lambda_3}\right)^3 - \frac{3}{2}(\gamma + 1)M_\infty^2 \tau y_2 \sqrt{\lambda_3} = \sqrt{\lambda_\infty^3} + 3(\gamma + 1)M_\infty^2 \tau \left(x_2 + \frac{1}{2} y_2 \sqrt{\lambda_2} \right). \tag{31}$$

For the first iteration step, we set $\lambda_3 \approx \lambda_2$. Only the value in the neighborhood of λ_2 is of interest. With equations (30) and (29) first μ_3 and then x_3 can be calculated.

Beginning step.– In this special case a compression shock appears as boundary value (fig. 4). The points P_1 and P_3 lie on the shock wave. The state variables for the new point P_3 must be identical with those from P_2. Once again, only the location remains to be established, just as with the general step. The mean value of the Mach line inclination before and behind the front is used for the inclination of the shock, so that the calculation of the spatial coordinates of P_3 involves no difficulties. Hence, for this purpose, only the closed formulas are involved:

$$x_3 = \frac{\sqrt{\lambda_3}(2\sqrt{\lambda_\infty} + \sqrt{\lambda_3} + \sqrt{\lambda_1})}{2\sqrt{\lambda_\infty} - 3\sqrt{\lambda_3} + \sqrt{\lambda_1}} \left[y_1 - y_2 + \frac{x_2}{\sqrt{\lambda_3}} - \frac{4x_1}{2\sqrt{\lambda_\infty} + \sqrt{\lambda_3} + \sqrt{\lambda_1}} \right]; \tag{32}$$

$$y_3 = y_2 + \frac{1}{\sqrt{\lambda_3}}(x_3 - x_2). \tag{33}$$

4. The non-stationary flow field

After the stationary flow field is known at individual points, the non-stationary problem can be approached. Eq. (7) must now be solved with the boundary condition

eq. (10). The theory of characteristics will also be brought in for this. Only factors of the highest derivatives have an influence on the directional conditions. Since these factors for ψ_{xx} and ψ_{yy} agree with those of Φ_{xx} and Φ_{yy} in eq. (6), the same directions for the Mach lines are found as in the stationary flow field. The network of characteristics in the current plane is also unchanged and can be taken over completely from the stationary problem. For the derivation of the new consistence relations, the second-order differential equation, eq. (7), must be transformed into a system of two first-order differential equations. New symbols are therefore introduced for the derivation:

$$\psi_x = U; \quad \psi_y = V. \tag{34}$$

In addition, eq. (13) should be considered. The following system of equations is /344
then obtained:

$$\begin{cases} \lambda U_x - V_y + \left(\lambda_x + 2i\frac{\omega}{U_\infty} M_\infty^2\right) U - \frac{\omega^2}{c_\infty^2}\psi = 0. \\ U_y - V_x = 0. \end{cases} \tag{35}$$

It is easy to convince oneself that the second line of eq. 35 is true. In order to bring the system into "characteristic form", the perturbation quantities must be differentiated along the characteristics. For an arbitrary function f:

$$\left(\frac{\partial f}{\partial z}\right)_{\xi,\eta} = \frac{\partial f}{\partial x} \pm \frac{1}{\sqrt{\lambda}}\frac{\partial f}{\partial y}, \tag{36}$$

or, inversely:

$$\begin{cases} \frac{\partial f}{\partial x} = \frac{1}{2}\left[\left(\frac{\partial f}{\partial z}\right)_\xi + \left(\frac{\partial f}{\partial z}\right)_\eta\right]; \\ \frac{\partial f}{\partial y} = \frac{\sqrt{\lambda}}{2}\left[\left(\frac{\partial f}{\partial z}\right)_\xi - \left(\frac{\partial f}{\partial z}\right)_\eta\right]. \end{cases} \tag{37}$$

These operations are carried out in eq. (35). After a short calculation the result is:

$$\begin{cases} \sqrt{\lambda}\left[\left(\frac{\partial U}{\partial x}\right)_\xi + \left(\frac{\partial U}{\partial x}\right)_\eta\right] - \left[\left(\frac{\partial V}{\partial x}\right)_\xi - \left(\frac{\partial V}{\partial x}\right)_\eta\right] + \frac{2}{\sqrt{\lambda}}\left[\left(\lambda_x + 2i\frac{\omega}{U_\infty} M_\infty^2\right) U - \frac{\omega^2}{c_\infty^2}\psi\right] = 0; \\ \sqrt{\lambda}\left[\left(\frac{\partial U}{\partial x}\right)_\xi - \left(\frac{\partial U}{\partial x}\right)_\eta\right] - \left[\left(\frac{\partial V}{\partial x}\right)_\xi + \left(\frac{\partial V}{\partial x}\right)_\eta\right] = 0. \end{cases} \tag{38}$$

By addition and subtraction the new consistency relations can be found. At the same time, the substitution of eq. (34) is regressively made:

$$\left(\frac{\partial \Psi_x}{\partial x}\right)_{\xi,\eta} \mp \frac{1}{\sqrt{\lambda}}\left(\frac{\partial \Psi_y}{\partial x}\right)_{\xi,\eta} + \frac{1}{\lambda}\left(\lambda_x + 2i\frac{\omega}{U_\infty} M_\infty^2\right)\psi_x - \frac{1}{\lambda}\frac{\omega^2}{c_\infty^2}\psi = 0. \tag{39}$$

As indicated in the first section, the nonlinear theory only needs to be applied for small reduced frequencies. For this reason, the terms with ω^2 could be neglected. This results in a few simplifications in the calculation. With the method derived here, these terms cannot be discarded. It has namely been shown that the reduced frequency must be very small if the ω^2 term is to be ignored in eq. (39) for the determination of the pressure distribution.

This equation has a boundary condition:

$$y = 0: \quad \psi_y = \frac{dh_2}{dx} + i\frac{\omega}{U_\infty} h_2. \tag{40}$$

In order to calculate the bow wave, the shock poles must be included. The explicit formulas can be taken directly from [11]. Hence, the details of their derivation will not be gone into here. Values of ψ_x and ψ_y directly behind the shock front are indicated by a caret over the symbol. In terms of the function G, which was related to the spreading out of the shock, one obtains:

$$\begin{cases} \hat{\psi}_x = m_1 \frac{dG}{dy} + i m_2 G; \\ \hat{\psi}_y = n_1 \frac{dG}{dy} + i n_2 G. \end{cases} \tag{41}$$

where the following definitions have been used:

$$\begin{cases} m_1 = \frac{2}{\gamma+1} \frac{\sqrt{\hat{\lambda}}+\sqrt{\lambda_\infty}}{\left[1+\left(\frac{\sqrt{\hat{\lambda}}+\sqrt{\lambda_\infty}}{2}\right)^2\right]^2}; \\ m_2 = \frac{8}{\gamma+1} \frac{1}{1+\left(\frac{\sqrt{\hat{\lambda}}+\sqrt{\lambda_\infty}}{2}\right)^2} \frac{\omega}{U_\infty} \left[1 + \frac{1+\left(\frac{\sqrt{\hat{\lambda}}+\sqrt{\lambda_\infty}}{2}\right)^2}{M_\infty^2}\right]; \\ n_1 = -\frac{U_\infty}{\omega} m_2 + \frac{2}{\sqrt{\hat{\lambda}}+\sqrt{\lambda_\infty}} m_1; \\ n_2 = -\frac{1}{2}\left(\sqrt{\hat{\lambda}}+\sqrt{\lambda_\infty}\right) m_2. \end{cases} \tag{42}$$

The function G, multiplied by $\exp(i\omega t)$, gives the deflection of the central position of the front. The quantities m_1, m_2, n_1 and n_2 depend only on the frequency and the value of the stationary field. If the stationary field is known, they can be calculated. Only $G(y)$ remains unknown, then, on the right-hand side of eq. (41). Further particulars may be found in [11].

THE SPECIAL STEPS.– Just as in the stationary procedure, three special cases are distinguished. First of all, certain transformations can be employed for the calculation of the angular points, taking into consideration that along the left-hand characteristics values of the stationary state variables remain constant. Here the consistency relations along the appropriate Mach lines should be specially treated. Eq. (39) holds with the upper sign for the left-hand characteristic ξ=const. With corrected differentiation the relation reads

$$\left(\frac{\partial \psi_x}{\partial \eta}\right)_\xi - \frac{\tau}{\sqrt{\lambda}}\left(\frac{\partial \psi_y}{\partial \eta}\right)_\xi + \frac{\lambda_x}{\lambda}\psi_x\left(\frac{\partial x}{\partial \eta}\right)_\xi + 2i\frac{\omega}{U_\infty}M_\infty^2\frac{\psi_x}{\lambda}\left(\frac{\partial x}{\partial \eta}\right)_\xi - \frac{1}{\lambda}\frac{\omega^2}{c_\infty^2}\psi\left(\frac{\partial x}{\partial \eta}\right)_\xi = 0. \tag{43}$$

The values of λ can be taken directly from the results for the stationary flow field. The derivative λ_y should be transformed in such a way that derivatives along the characteristics now appear: /346

$$\lambda_x = \lambda_\xi \cdot \xi_x + \lambda_\eta \cdot \eta_x. \tag{44}$$

But λ is independent of η, so that λ_η vanishes. ξ and η should then be replaced by x and y:

$$\lambda_x = \lambda_\xi \cdot \xi_x = \lambda_\xi \frac{\frac{1}{x_\xi}}{1 - \frac{x_\eta}{x_\xi}\frac{y_\xi}{y_\eta}}. \tag{45}$$

After consideration of eq. (11) the denominator takes the value 2, so that finally:

$$\lambda_x = \frac{1}{2}\frac{\lambda_\xi}{x_\xi} = \frac{1}{2}\left(\frac{\partial \lambda}{\partial x}\right)_\eta. \tag{46}$$

Furthermore, the potential function ψ is reduced to its derivatives. From the definition:

$$\left(\frac{\partial \psi}{\partial x}\right)_\xi = \psi_x + \frac{1}{\sqrt{\lambda}}\psi_y \tag{47}$$

and through integration the following results:

$$\psi = \psi_a + \int_{\xi=const.}\left(\psi_x + \frac{1}{\sqrt{\lambda}}\psi_y\right)dx \tag{48}$$

wherein the integration path lies along ξ=const. ψ_a denotes a constant of integration. Finally one obtains, for the left-hand characteristic:

$$d\psi_y - \frac{1}{\sqrt{\lambda}} d\psi_y + \frac{1}{2}\frac{\psi_x}{\lambda}\left(\frac{\partial \lambda}{\partial x}\right)_\eta dx + 2i\frac{\omega}{U_\infty} M_\infty^2 \frac{\psi_x}{\lambda} dx - \frac{\omega^2}{U_\infty^2} M_\infty^2 \frac{dx}{\lambda}\left[\psi_a + \int_{\xi=const.}\left(\psi_x + \frac{1}{\sqrt{\lambda}}\psi_y\right) dx\right] = 0. \tag{49}$$

The differentials should likewise be taken along ξ=const. The procedure for the right-hand characteristic is exactly analogous. Consistency relations for η=const. can be written as follows:

$$\left(\frac{\partial \psi_x}{\partial \xi}\right)_\eta - \frac{1}{\sqrt{\lambda}}\left(\frac{\partial \psi_y}{\partial \xi}\right)_\eta + \frac{\psi_x}{\lambda}\lambda_x\left(\frac{\partial x}{\partial \xi}\right)_\eta + 2i\frac{\omega}{U_\infty} M_\infty^2 \frac{\psi_x}{\lambda}\left(\frac{\partial x}{\partial \xi}\right)_\eta - \frac{\omega^2}{U_\infty^2} M_\infty^2 \frac{\psi_x}{\lambda}\left(\frac{\partial x}{\partial \xi}\right)_\eta = 0. \tag{50}$$

This time the expression $\lambda_x\left(\frac{\partial x}{\partial \xi}\right)_\eta$ should be further transformed:

$$\lambda_x \cdot x_\xi = \lambda_\xi \cdot \xi_x \cdot x_\xi = \lambda_\xi \frac{1}{1 - \frac{\eta_x}{\eta_y}\frac{\xi_y}{\xi_x}}. \tag{51}$$

In place of x and y, ξ and η should again be introduced. The result is then

$$\lambda_x \cdot x_\xi = \frac{1}{2}\left(\frac{\partial \lambda}{\partial \xi}\right)_\eta. \tag{52}$$

For the integration of the potential function ψ there is now:

$$\psi = \psi_b + \int_{\eta=const.}\left(\psi_x - \frac{1}{\sqrt{\lambda}}\psi_y\right) dx, \tag{53}$$

where ψ_b is again a constant of integration. Eq. (50) can then be rewritten:

$$d\psi_x + \frac{1}{\sqrt{\lambda}} d\psi_y + \frac{1}{2}\frac{\psi_x}{\lambda} d\lambda + 2i\frac{\omega}{U_\infty} M_\infty^2 \frac{\psi_x}{\lambda} dx - \frac{\omega^2}{U_\infty^2} M_\infty^2 \frac{\psi_x}{\lambda}\left[\psi_b + \int_{\eta=const.}\left(\psi_x - \frac{1}{\sqrt{\lambda}}\psi_y\right) dx\right] = 0. \tag{54}$$

Naturally, all differentials in eq. (54) must be performed along η=const.

a. General Step.– To illustrate the procedure, the difference form for a characteristic will be explicitly written out. The location of the singular point is known. The right-hand Mach line P_1P_2 (fig. 2) is chosen as an example. For the analysis of the

term with ω^2 in eq. (54), only ψ_1 need enter for ψ_b. In an explicit representation this equation reads (U and ψ_x are identical, as are V and ψ_y):

$$U_3 - U_1 + \frac{2}{\sqrt{\lambda_3}+\sqrt{\lambda_1}}(V_3 - V_1) + \frac{U_3+U_1}{\lambda_3+\lambda_1}\left[\frac{1}{2}(\lambda_3-\lambda_1) + 2i\frac{\omega}{U_\infty}M_\infty^2(x_3-x_1)\right] - 2\frac{\omega^2}{U_\infty^2}M_\infty^2\frac{x_3-x_1}{\lambda_3-\lambda_1}\left[\psi_1 + (x_3-x_1)\left(\frac{U_3+U_1}{2} - \frac{V_3+V_1}{\sqrt{\lambda_3}+\sqrt{\lambda_1}}\right)\right] = 0. \quad (55)$$

For the left-hand characteristic, eq. (49) must be written out. ψ_a is replaced by ψ_2. There result two complex, linear equations for U_3 and V_3. It must further be considered that both desired quantities consist of real and imaginary parts, and it is necessary to solve a linear system of equations consisting of four equations. This presents no difficulty. Since the analytic results cannot be written in an elegant way, their detailed /348
form will be dispensed with. Because the entire calculation will be carried out on an electronic calculating machine, it seems advantageous to have the values of the stationary flow field of a point occur directly before the calculation of the additional non-stationary quantities. In this way the memory capacity of the machine will not be unnecessarily taxed.

b. Boundary conditions.– Since the location of the point for which the non-stationary ensemble quantities are sought is known, a great simplification enters compared to the stationary problem. It is no longer necessary to carry out an iteration. Since the value of ψ_y is given by eq. (40), it remains only to solve eq. (54) for the unknown ψ_x, which however involves no difficulties.

c. Beginning step.– Eqs. (41) are brought in as the shock poles. In setting up the equation along ξ=const. one must proceed somewhat carefully (fig. 5). In the third term of eq. (49) there is a factor $\left(\frac{\partial\lambda}{\partial x}\right)_\eta$. A right-hand characteristic from the region behind the shock, however, does not run into P_3. In this case this gradient should

be constructed at another point, at P_{23}, lying between P_2 and P_3. The slope of the right-hand characteristic at P_{23} can be simply ascertained. The relationship for the gradient reads

$$\left(\frac{\partial\lambda}{\partial x}\right)_\eta = \frac{\lambda_{23} - \lambda_{13}}{x_{23} - x_{13}}. \tag{56}$$

Further conditions are given by

$$\lambda_{23} = \lambda_3; \quad x_{33} = \frac{1}{2}(x_3 + x_2). \tag{57}$$

The characteristic $P_{23}P_{13}$ can be taken to be approximately parallel to P_1P_2. With small step sizes this is completely justified. The same justification lies behind the linear distribution of λ between P_1 and P_3. The following relations are then obtained:

$$\lambda_{13} = \frac{1}{2}(\lambda_3 + \lambda_1); \qquad x_{13} = \frac{1}{2}(x_3 + x_1). \tag{58}$$

With eq. (56), (57) and (58), $\left(\frac{\partial\lambda}{\partial x}\right)_\eta$ can now be calculated:

$$\left(\frac{\partial\lambda}{\partial x}\right)_\eta = \frac{\lambda_3 - \lambda_1}{x_3 - x_1}. \tag{59}$$

This gradient will be brought in for the construction of the characteristic conditions, eq. (49).

The detailed construction of the difference form will again be dispensed with, since the methodology was already explained for eq. (55).

5. The Characteristic Field

The entire calculation of the characteristic field can be reduced to the special steps quoted above. An exception to this is the first step of the calculation. This point P_0 (fig. 1) lies as much on the shock curve as on the body. The value for λ can be calculated for the stationary field with eq. (15) at a known location and hence a given μ. For the determination of the non-stationary quantities the following are needed: (i) the shock poles, eq. (41); and (ii) the boundary conditions, eq. (40).

Vibrational oscillations are denoted by:

$$h_2 = k_1 = const. \tag{60}$$

The data for the starting point P_0 then are:

$$\begin{cases} \bar{\psi}_x = 0; & \bar{\bar{\psi}}_x = \frac{m_1}{n_1}\frac{\omega}{U_\infty}k_1; \\ \bar{\psi}_y = 0; & \bar{\bar{\psi}}_y = \frac{\omega}{U_\infty}k_1; \\ \bar{G} = 0; & \bar{\bar{G}} = 0. \end{cases} \tag{61}$$

Singly barred quantities denote the real part, while doubly barred quantities denote the imaginary part. For the torsional oscillation, h_2 is given as proportional to x:

$$h_2 = k_1(x - x_C). \tag{62}$$

x_C is the coordinate of the center of rotation. At the point P_0 the result is

$$\begin{cases} \bar{\psi}_x = \frac{m_1}{n_1}k_1; & \bar{\bar{\psi}}_x = \frac{m_1}{n_1}\frac{\omega}{U_\infty}k_1(x - x_C); \\ \bar{\psi}_y = k_1; & \bar{\bar{\psi}}_y = \frac{\omega}{U_\infty}k_1(x - x_C); \\ \bar{G} = 0; & \bar{\bar{G}} = 0. \end{cases} \tag{63}$$

With these relationships for the initial point on the profile, the calculation can be begun.

6. Results

As an example, vibrational and torsional oscillations for parabolic profiles (fig. 6) were calculated. The Mach number of the incident flow amounts to $M_\infty = 1.2$. In order to have another supersonic field behind the desired compression shock, the thickness ratio may only be changed to about $\tau = 0.025$. With greater incident Mach numbers, the maximum value of τ will likewise be higher.

First, the pressure coefficients were calculated at a constant reduced frequency k, which was constructed with half of the profile length, and with a varying τ. Here, the influence of the thickness ratio was investigated (fig. 7) relative to the linear theory ($\tau = 0$). The pressure coefficient is given by

$$C_p = \tilde{C}_p e^{i\omega t} = -2(\psi_x + ik\psi)e^{i\omega t}. \tag{64}$$

The real and imaginary parts the of amplitude function $\tilde{C}_p$ are given by

$$\begin{cases} \Re e(\tilde{C}_p) = \overset{\sim}{\tilde{C}}_p = -2(\bar{\psi}_x - k\bar{\bar{\psi}}); \\ \Im m(\tilde{C}_p) = \overset{\approx}{\tilde{C}}_p = -2(\bar{\bar{\psi}} + k\bar{\psi}). \end{cases} \tag{65}$$

$\overset{\sim}{\tilde{C}}_p$ and $\overset{\approx}{\tilde{C}}_p$ are shown in figures 7a and 7b for vibrational oscillations. For the abscissa the profile chord, stretching from $-1 \leq x \leq 1$, was used. With respect to the real part $\overset{\sim}{\tilde{C}}_p$, it can be seen that the maximum moves forward from the back edge with increasing τ. The somewhat diminished value at $\tau = 0.025$ indicates that calculations there should perhaps be more exact. The step sizes for all examples were so chosen that the change from point to point would not exceed a certain amount. In this way /353
there was a variable step size not just at different values of τ, but also with a single τ within the characteristic field. In order to limit expenses that amount was so chosen that a boundary point was determined about 13 to 14 times. The average step size was about $0.13\ l$, where l is again half of the profile length. The values from about 13-14 points at a time result in a single curve in figure 7. The same step sizes were also retained for the calculation of the torsional oscillations.

The differences from the linear theory are not so evident with the imaginary part $\overset{\approx}{\tilde{C}}_p$ (fig. 7b). Still, some influence of thickness is found here as well, in the momentum coefficients.

In figure 8 the pressure distributions for constant τ and variable frequency k are shown. The incident flow Mach number is once again $M_\infty = 1.2$. A greater waviness appears, due to the increased frequency. Comparisons with the linear theory, which is shown in dashed lines, show that here also the pressure maxima are more pronounced. Similar tendencies are already indicated by the second-order theory [14]. The pressure coefficients $\tilde{C}_p$ are shown in figure 9 for $M = 1.4$ and $\tau = 0.04$. The linear theory for $k = 0.3$ is given for comparison.

Of great interest are also the rise in buoyancy and the dependence of the momentum

curve on the thickness ratio and the reduced frequency. For this purpose, different integrals must be constructed:

$$L = 2\int_{-1}^{+1} \tilde{C}_p \, dx; \tag{66}$$

$$M = 2\int_{-1}^{+1} \tilde{C}_p x \, dx; \tag{67}$$

Eq. (66) and eq. (67) form the amplitudes for the force and momentum of an oscillating profile. For comparison with the linear theory, the following relations for buoyancy and momentum are taken from [15]:

$$\frac{dc_L}{d\alpha_h} = i\frac{1}{4k}\left(\bar{\bar{L}} + i\bar{\bar{L}}\right) \quad \text{(vibrational oscillations)}; \tag{68}$$

$$\frac{dc_M}{d\alpha_h} = -i\frac{1}{4k}\left(\bar{\bar{M}} + i\bar{\bar{M}}\right) \quad \text{(vibrational oscillations)}; \tag{69}$$

Single barred quantities denote the real part, doubly barred quantities the imaginary part. The first formula is related to the buoyancy coefficient c_L, eq. (69) is related to the momentum coefficient c_M.

In figure 10 the rise in the buoyancy curve and its phase angle θ_h for vibrational oscillations is drawn as a function of the reduced frequency. The incident Mach number amounts to $M_\infty = 1.2$, just as with the following figures. For comparison the results of the linear theory ($\tau = 0$) are given as dashed lines. It appears that the influence of the thickness ratio is very small. These statements are confirmed by the second order theory [14]. The rise in the momentum curve and its phase angle θ_{hM} are exhibited in figure 11. The center of the profile was chosen for the momentum reference pole. A strong dependence on τ is established with these curves. The considerable deviations with respect to the phase angle are rooted in the different boundary value considerations. For the linear theory, first the limit $\tau \to 0$ is taken, and then $k \to 0$. If the two limiting procedures were reversed, the relation $\theta_{hM} = 0$ would result.

/355

/356

/358–
359

The results for torsional oscillations about the profile center are shown in the /358
following figures. In figures 12a and 12b, the influence of the thickness ratio τ with
constant k is illustrated. While for the real part the variation in τ is only noticeable /359
at the forward edge, the imaginary part reflects a marked dependence on τ. Even here, the step sizes for $\tau = 0.025$ appear to have again been chosen too large. At the same time, it must likewise be considered that one is near to the boundary, where the shock detatches itself from the profile.

In order to investigate the dependence on k, the pressure distribution at $\tau = 0.02$ is presented in figures 13a and 13b. One sees that with increasing frequency the curves gain a greater waviness. Compared to the linear theory, whose results are again shown as dashed lines, larger pressure maxima appear at the forward edge, while in the back part of the profile not such high values are reached. A partial reason for this can certainly be sought in the fact that a compression shock exists at the profile.

In analogy with eq. (68) and (69), the buoyancy and the momentum curves can be determined. The rises are calculated as follows:

$$\frac{dc_L}{d\alpha} = \frac{1}{4k}\left(\bar{L} + i\bar{\bar{L}}\right) \qquad \text{(Rotational oscillation);} \tag{70}$$

$$\frac{dc_M}{d\alpha} = -\frac{1}{4k}\left(\bar{M} + i\bar{\bar{M}}\right) \qquad \text{(Rotational oscillation).} \tag{71}$$

In figure 14 the absolute value and the phase angle θ_α of eq. (70) are now presented, as a function of the reduced frequency. Here again one sees that only relatively small deviations with respect to the linear theory appear. At the rise in the momentum curve, however – absolute value and phase angle are represented in figure 15 – significant deviations from the linear theory result. Just as in figure 11, the different boundary limiting procedures are influential in the large difference of $\theta_{\alpha M}$ with small reduced frequencies.

/360

7. Summary.

Non-stationary supersonic flow in the near-sonic range is calculated. A perturbation based on the exact stationary values is assumed for the nonlinear potential equation. In this way the problem can be divided into the separate calculation of the stationary and of the non-stationary field. The pressure distribution for an oscillating profile is determined by a characteristics procedure. In order to ba able to use such a method, the initial differential equations must be of hyperbolic type. This means that the compression shock must lie at the peak of the profile. For a profile with a given thickness ratio, then, the supersonic Mach number must be above a certain value. Another problem then appears if the stationary part observes a Mach number /360
of the desired boundary value, while the non-stationary addition brings the value of the local Mach number under one. In this case the procedure cannot be used.

Certain statements on the applicability of the linear theory are important. Next it is to be established that only for very small frequencies can the term in the differential equation with ω^2 be canceled. Up to high values of the reduced frequency, where the non-linear, near-sonic theory can be replaced by an explicitly linear one, the calculations have not been carried out. From different figures one can perhaps extrapolate, so that the linear theory can be used for calculation to about $k \sim 0.8$. For ascertaining the buoyancy coefficients there are no evident differences at small frequencies. However, for the momentum coefficients considerable mistakes would enter in. In this case it is better to determine the coefficients oneself for very small thickness ratios with the procedure delineated here.

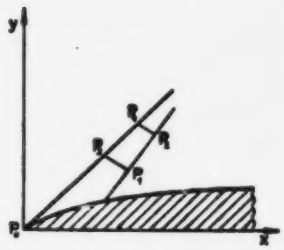

Figure 1. Bow wave at the profile

Figure 2. General step

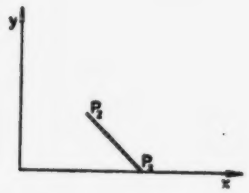

Figure 3. Edge step

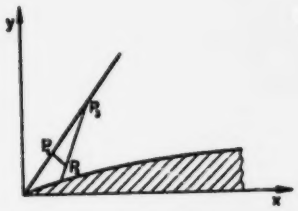

Figure 4. Beginning step

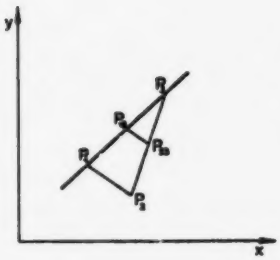

Figure 5. Beginning step for the non-stationary problem

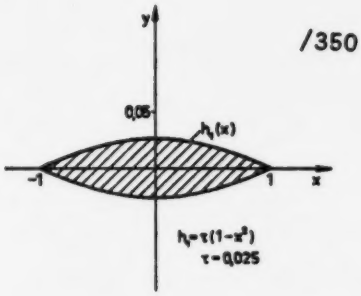

Figure 6. Given profile

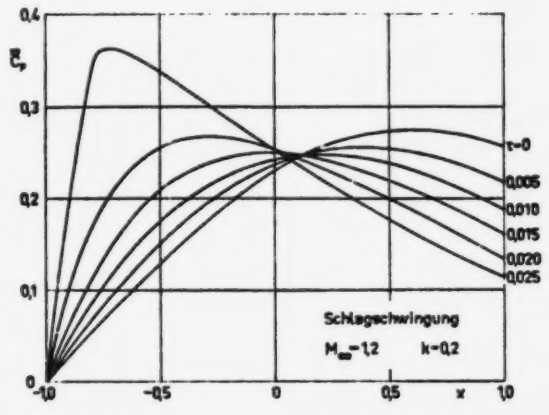

Figure 7a. Pressure distribution $\bar{\bar{C}}_p$ (real part) for a parabolic curve profile at the reduced frequency $k = 0.2$ (parameter: thickness ratio τ). Vibrational oscillation $M_\infty = 1.2$

ORIGINAL PAGE IS
OF POOR QUALITY

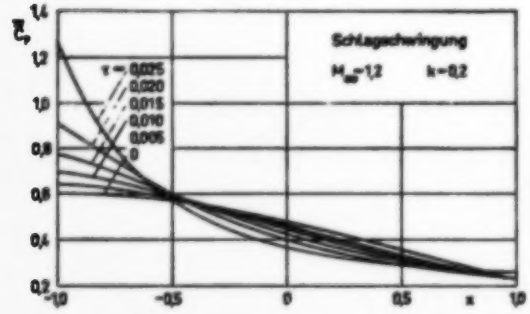

/351

Figure 7b. Pressure distribution $\tilde{\tilde{C}}_p$ (imaginary part) for a parabolic curve profile at the reduced frequency $k = 0.2$ (parameter: thickness ratio τ) Vibrational oscillation $M_\infty = 1.2$

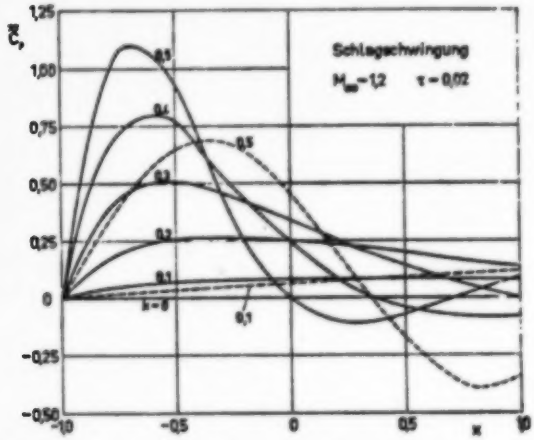

/352

Figure 8a. Pressure distribution $\tilde{\tilde{C}}_p$ (real part) for a parabolic curve profile with the thickness ratio $\tau = 0.02$ (parameter: reduced requency k). Vibrational oscillation $M_\infty = 1.2$

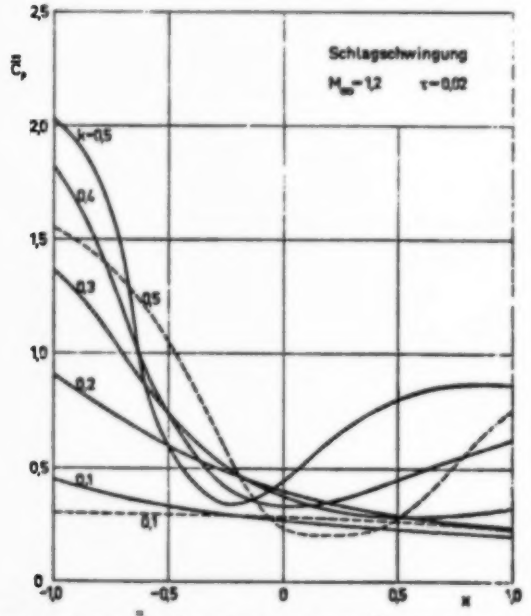

/352

Figure 8b. Pressure distribution $\tilde{\tilde{C}}_p$ (imaginary part) for a parabolic curve profile with the thickness ratio $\tau = 0.02$ (parameter: reduced frequency k) Vibrational oscillation $M_\infty = 1.2$

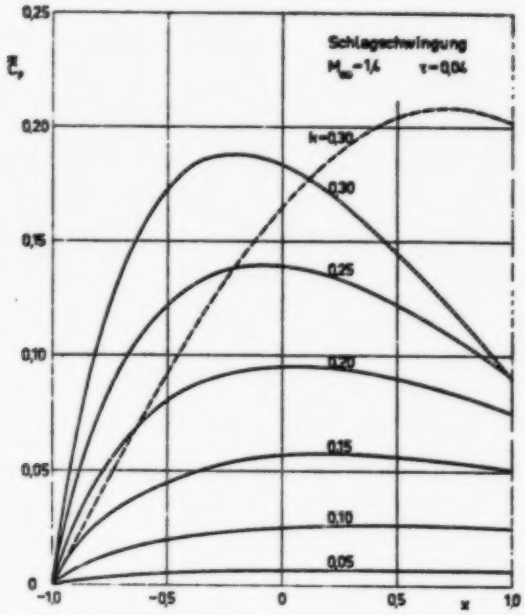

/354

Figure 9a. Pressure distribution $\bar{\bar{C}}_p$ (real part) for a parabolic curve profile with the thickness ratio $\tau = 0.04$ (parameter: reduced requency k). Vibrational oscillation $M_\infty = 1.4$

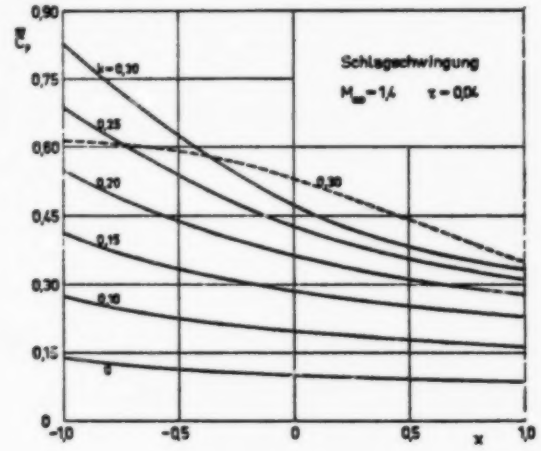

/354

Figure 9b. Pressure distribution $\bar{\bar{C}}_p$ (imaginary part) for a parabolic curve profile with the thickness ratio $\tau = 0.04$ (parameter: reduced frequency k) Vibrational oscillation $M_\infty = 1.4$

/355

ORIGINAL PAGE IS
OF POOR QUALITY

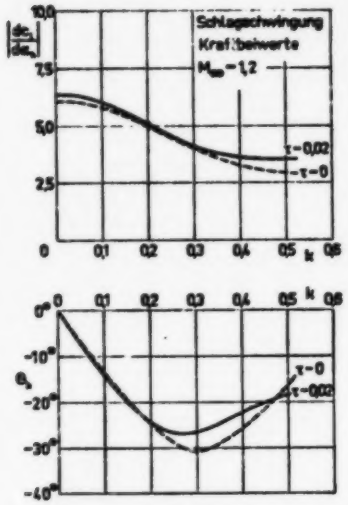

Figure 10. Buoyancy coefficients for vibrational oscillations

/355

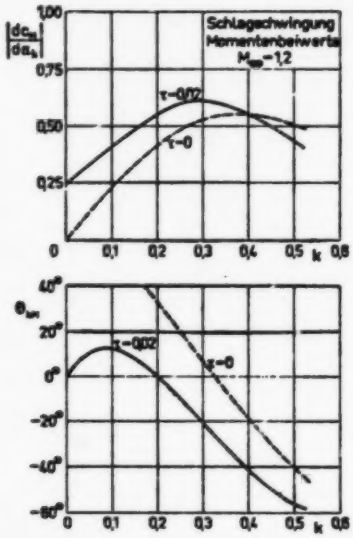

Figure 11. Momentum coefficients for vibrational oscillations

/356

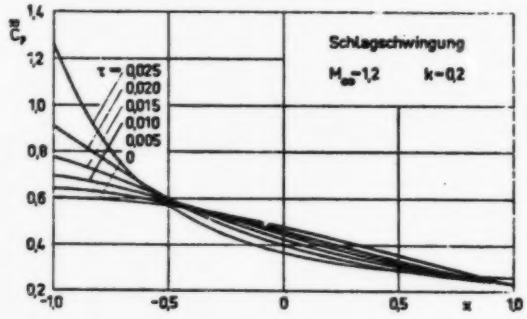

Figure 12a. Pressure distribution $\tilde{C}_p$ (real part) for a parabolic curve profile at the reduced frequency $k = 0.2$ (parameter: thickness ratio τ). Vibrational oscillation $M_\infty = 1.2$

ORIGINAL PAGE IS
OF POOR QUALITY

/356

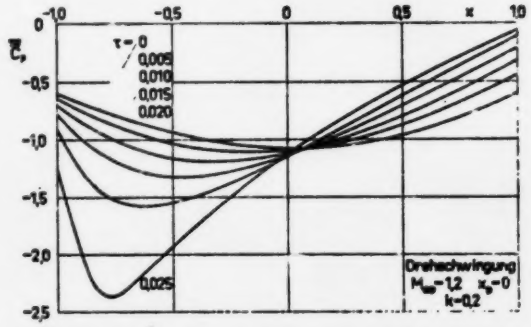

Figure 12b. Pressure distribution $\bar{\bar{C}}_p$ (imaginary part) for a parabolic curve profile at the reduced frequency $k = 0.2$ (parameter: thickness ratio τ) Torsional oscillation $M_\infty = 1.2$, $x_C = 0$

/357

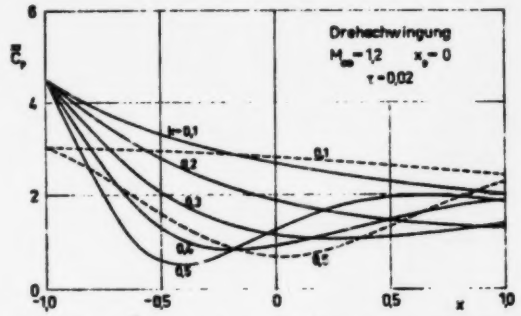

Figure 13a. Pressure distribution $\bar{\bar{C}}_p$ (real part) for a parabolic curve profile with the thickness ratio $\tau = 0.02$ (parameter: reduced requency k). Torsional oscillation $M_\infty = 1.2$, $x_C = 0$

/357

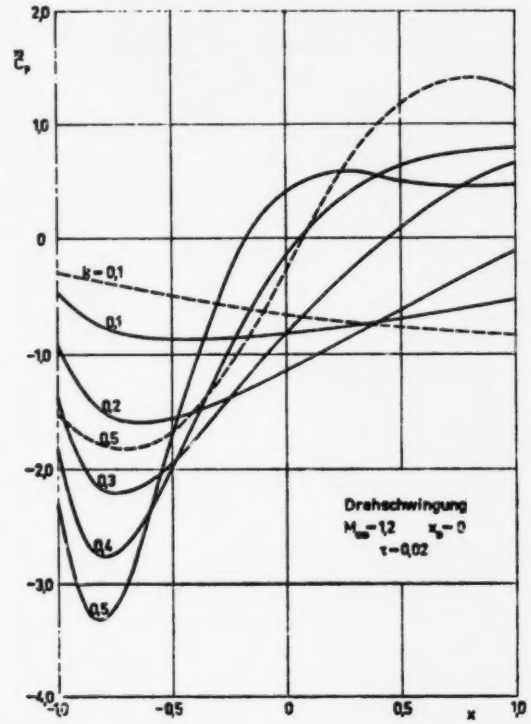

Figure 13b. Pressure distribution $\bar{\bar{C}}_p$ (imaginary part) for a parabolic curve profile with the thickness ratio $\tau = 0.02$ (parameter: reduced frequency k) Torsional oscillation $M_\infty = 1.2$, $x_C = 0$

ORIGINAL PAGE IS
OF POOR QUALITY

/358

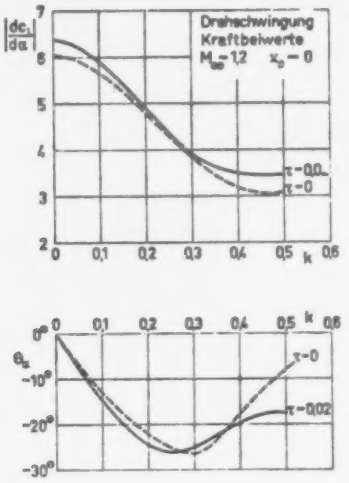

Figure 14. Buoyancy coefficients for torsional oscillations

/357

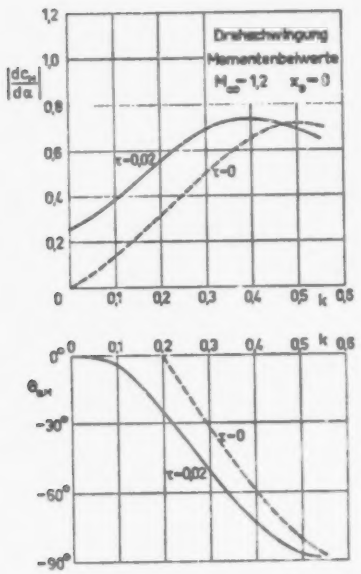

Figure 15. Momentum coefficients for torsional oscillations

REFERENCES

[1] Lin C. C., Reissner E. and Tsien H. S., *On two-dimensional non-steady motion of a slender body in a compressible fluid* (*J. Math. Phys.*, vol. 25, 1948, p. 220-231).

[2] Hayes W. D., *On hypersonic similitude* (*Quart. Appl. Math.*, vol. 5, 1947, p. 105).

[3] Lighthill M. J., *Oscillating airfoils at high Mach-number* (*J. Aero. Sc.*, vol. 20, 1953, p. 402-406).

[4] Coupry G. et Piazollio., *Étude du flottement en régime transsonique* (*Rech. Aéro.*, nº 63, 1958, p. 19-28).

[5] Eckhaus W., *Two-dimensional, transonic unsteady flow with shock-waves*, O. S. R., TN, Nr. 59-491, mai 1959.

[6] Hosokawa I., *A simplified analysis for transonic flows around thin bodies* (*Symposium Transsonicum*, Springer Verlag, Berlin, 1964, p. 184-199).

[7] Teipel I., *Die instationären Luftkräfte bei der Machzahl* 1 (*Symposium Transsonicum*, Springer Verlag, Berlin, 1964, s. 457-459).

[8] Landahl M. T., *Unsteady Transonic Flow*, Pergamon Press, New York, 1961.

[9] Oswatitschs K., *Similarity and Equivalence in Compressible Flow* (*Adv. Appl. Mech.*, vol. 6, Academic Press, New York, 1960).

[10] Spreiter J., *On the alternative forms for the basic equations of transonic flow theory* (*J. Aero. Sc.*, vol. 21, 1954, p. 70-72).

[11] Teipel I., *Die Verdichtungsstosswelle an einem oszillierenden Keil* DVL-Bericht Nr 424.

[12] Oswatitsch K., *Die Berechnung wirbelfreier achsensymmetrischer Ueberschallfelder* (*österr. Ing-Archiv X*, Bd. 4, 1956, s. 359-382).

[13] Sauer R., *Anfangswertprobleme bei partiellen Differentialgleichungen*, Springer-Verlag, Berlin, 2, Aufl., 1958.

[14] Van Dyke M., *Supersonic fow past oscillating airfoils including nonlinear thickness effects*, N. A. C. A., TN 2982, 1953.

[15] Nelson H. C. und Berman J. H., *Calculations on the forces and moments for an oscillating wing-aileron combination in two-dimensional potential flow at sonic speed*, N. A. C. A., Rep. 1128, 1953.

(Manuscript from the 26th of March 1965.)